ARTICLE

Check for updates

Modest flooding can trigger catastrophic road network collapse due to compound failure

Shangjia Dong[1], Xinyu Gao[2], Ali Mostafavi[2] & Jianxi Gao [3,4 ✉]

Compound failures occur when urban flooding coincides with traffic congestion, and their impact on network connectivity is poorly understood. Firstly, either three-dimensional road networks or the traffic on the roads has been considered, but not both. Secondly, we lack network science frameworks to consider compound failures in infrastructure networks. Here we present a network-theory-based framework that bridges this gap by considering compound structural, functional, and topological failures. We analyze high-resolution traffic data using network percolation theory to study the response of the transportation network in Harris County, Texas, US to Hurricane Harvey in 2017. We find that 2.2% of flood-induced compound failure may lead to a reduction in the size of the largest cluster where network connectivity exists, the giant component, 17.7%. We conclude that indirect effects, such as changes in traffic patterns, must be accounted for when assessing the impacts of flooding on transportation network connectivity and functioning.

[1] Department of Civil and Environmental Engineering, University of Delaware, Newark, DE 19716, USA. [2] Zachry Department of Civil and Environmental Engineering, Texas A&M University, College Station, TX 77840, USA. [3] Department of Computer Science, Rensselaer Polytechnic Institute, Troy, NY 12180, USA. [4] Network Science and Technology Center, Rensselaer Polytechnic Institute, Troy, NY 12180, USA. ✉email: jianxi.gao@gamil.com

nfrastructure networks play essential roles in maintaining community access and supporting economic activities. The proper functioning of networks is, however, constantly challenged by two major stressors: rapid population growth and destructive urban flooding[1–7]. Population growth increases travel demand and cause congestion that degrades the service quality of road networks. In addition, global flood exposure is projected to increase by a factor of three by 2050 due to population growth and the development of economic assets in flood-prone areas[8]. The rising frequency of devastating caused by urban flooding and the significance of infrastructure in societal functioning together highlight the need for understanding the robustness of the flood-disrupted infrastructure network to prepare our cities for future urban growth and to mitigate exacerbated flood risk.

The transportation network, in particular, has been shown to be vulnerable to urban flooding disruptions[9–12] because floods perturb transportation system metastability, which can lead to an abrupt regime shift between different states[2,13,14]. Meanwhile, the scale and magnitude of flood disruptions are increasing due to climate change[15]. Climate change-induced sea-level rise further contributes to flooding vulnerability of the transportation network[16,17]. Transportation network robustness has received wide attention in the interdisciplinary disaster, engineering, and network science research in recent studies[18–22]. The majority of existing studies related to the robustness and resilience of infrastructure, so far, focus only on the impact of a single type of failure. Transportation network researchers, in particular, model disruption by modifying the topological or functional attributes of roads[23]. For example, the robustness of transportation networks during urban flooding has been examined by simulating topological changes such as road inundation[2,20,24], earthquake-induced road failure[21,25], and targeted attacks[26]. Additionally, functionality changes such as travel delay[27] and travel speed reduction[18,19,28] are used to model network failure and examine the transportation network efficiency and robustness.

In reality, the flooding can, however, cause both network structural failure (SF) (i.e., road inundation) and functional failure (FF) (i.e., reduced travel speed) that exacerbate the disaster-impacted network connectivity loss, and should thus both be considered in the network failure modeling. Specifically, urban flooding could result in the road closure and traffic rerouting that increases travel demand on other road segments, which eventually worsens congestion on links distant from flooded areas. Consequently, road inundation and traffic congestion could drastically raise indirect failures, whose link structure and functionality remain intact but are isolated from the rest of the transportation network. Taking the illustrative transportation network in Fig. 1a as an example, when only flooding is investigated (e.g., the five low-elevation roads), the largest connected cluster, namely giant component (GC), contains 14 links (73.7% of the network) as shown in Fig. 1b; when only congestion (e.g., the six congested roads) is studied, the GC has 13 links (68.4% of the transportation network), according to Fig. 1c. When flood and congestion are coupled in Fig. 1d, only four links are neither flooded nor congested but detached from the GC. The GC size decreases to 21.1%. We define the interplay among these three failure types as a compound failure. The illustrative case shows that the impact of compound failure on network robustness would be more catastrophic than the singular ones due to the amplification of the individual failures. This compound effect is a product of the fact that external perturbation such as flooding not only causes SF but also impacts the functionality of the rest of the network and results in indirect topological failure (TF). Such important compound nature-human-induced failures are, however, not explicitly considered in the disaster-disrupted transportation network robustness modeling. The limited investigation

and understanding of such compound failure could lead to the underestimation of flood-induced failures in road transportation networks.

A deeper understanding of urban flooding-induced compound failures in transportation networks is essential for improving their robustness and resilience in the face of population growth and exacerbated climate change. The goal of this study is to shed light on the transportation network robustness under the influence of compound failures during urban flooding. Understanding this complex relationship helps us better understand how the transportation network behaves during urban natural disasters and design concrete strategies for enhancing their robustness. We use a percolation modeling approach to examine the impact of compound failure on transportation network robustness. Percolation theory integrates statistical physics principles and graph theory to capture the phase transition of a network from connected to disconnected due to disruptions[3]. By removing nodes and links that represent network failure, we can identify the critical threshold at which the network experiences structural change as the GC (i.e., the largest connected cluster that maintains the most connectivity) breaks down into smaller components[29,30]. Since the link removal resembles network disruptions, utilization of percolation theory in empirical flood-disrupted transportation network robustness analysis can facilitate the understanding of the interplay between structural, functional, and topological failures. In particular, we use the link quality derived from the travel speed and speed limit as the criteria for link removal. We propose that the road whose speed performance does not meet the acceptable standard is considered a failure and thus removed from the network. To the best of our knowledge, no prior research has investigated the impact of the compound failures on transportation network robustness.

By examining the empirical flood data on the spatially disturbed transportation network, we show that modest floods can severely affect road transportation network robustness; such impact escalates rapidly as the extent of flooding increases. In particular, 72% of link removal will lead to the total network connectivity loss before Hurricane Harvey, but it only takes 48% link removal to achieve the same effect during Hurricane Harvey, despite a modest level of flooding (i.e., a maximum of 2.5% flood-induced road closure). In addition, flooding also leads to instability in network robustness as the critical percolation thresholds vary abnormally during Hurricane Harvey. The impact of flooding is validated by comparing no-flooding and random scenarios with observed connectivity. The findings identify new directions for understanding the robustness of stressed infrastructure networks against compound failures, with implications for urban planning, as well as for hazard risk mitigation and disaster management.

Results
Flood-disrupted Harris County transportation network during 2017 Hurricane Harvey. We investigated compound failures in the road transportation network in Harris County, Texas (USA), in the case of the 2017 Hurricane Harvey flooding (August 1–October 31). Hurricane Harvey made landfall in Texas on August 26, 2017, causing an estimated $125 billion in damage. We obtained traffic data (road traverse speed at 15-min intervals) for each major road in August (before Harvey), September (during & post Harvey), and October (after Harvey). Harris County's transportation network comprises 19,712 links and 15,390 nodes. The period termed during Harvey refers to the period when the network experiences hazardous impacts (e.g., wind, rainfall, and flood). Post-Harvey is the time when rainfall has ended but road blockage (e.g., inundation and debris) is still a major concern.
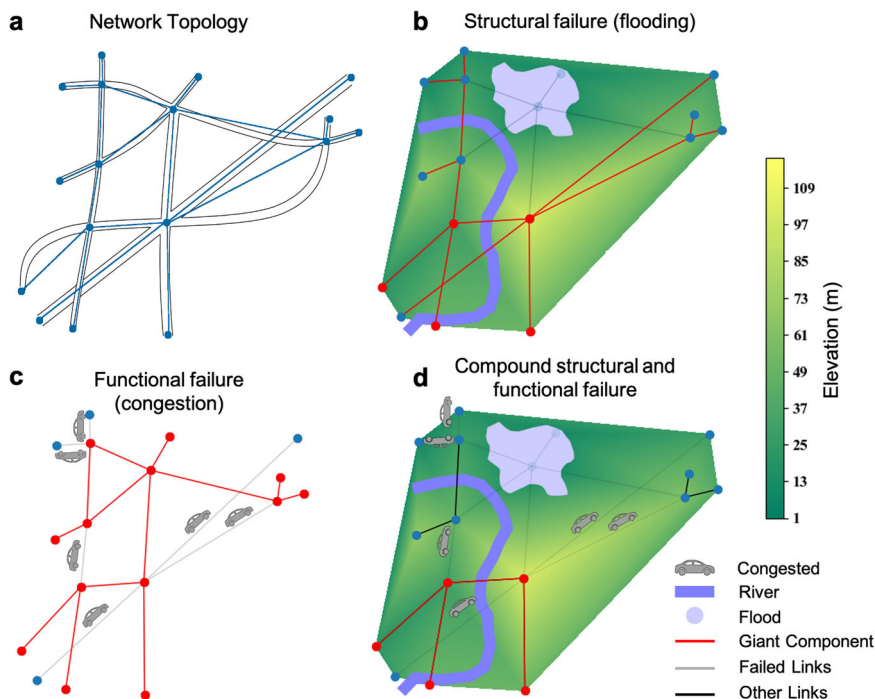
Fig. 1 Schematic diagram of flood impact on the transportation network. a Transportation network abstraction from roads to a graph with 19 links in total. **b** Transportation network in flooding (structural failure only, gray solid line). Low-elevation roads (five links) are flooded and marked as gray. The fourteen red links represent roads that are still connected to the giant component. **c** Transportation network in degraded service (i.e., congested) condition (functional failure only). Congestion here is defined as the link quality drops below the critical threshold. When certain roads are congested (six links with cars), they are considered to have low service quality, and their corresponding links (gray links) are removed from the giant component. **d** Transportation network under both structural and functional failures. The congested (low link quality) and flooded roads (six congested and five inundated) are marked as gray and removed from the network. The four black links represent the roads that are neither flooded nor congested but detached from the giant component.
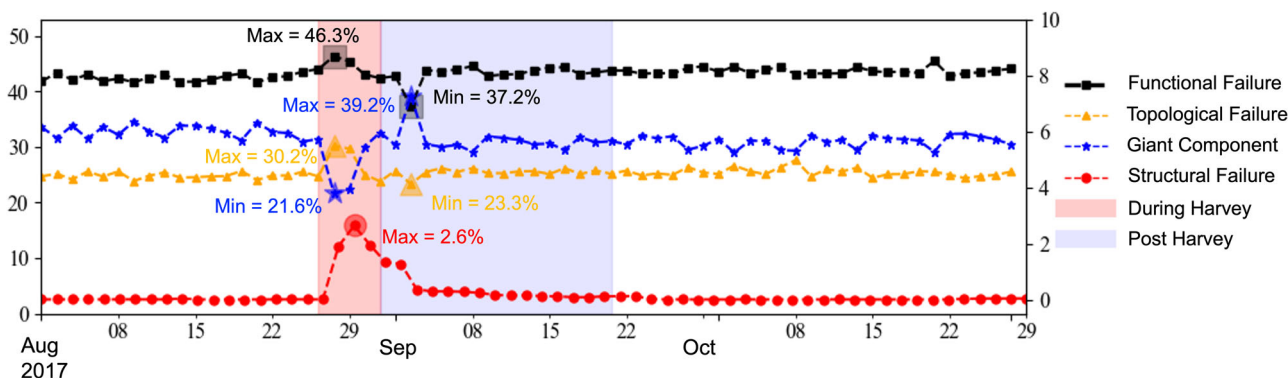

Fig. 2 Time series of individual failures and their evolution over the course of Hurricane Harvey. We use $q = 0.8$ for the illustrative purpose. The average failure before Harvey for each failure is a functional failure (42.3%) in black square solid line, topological failure (24.8%) in yellow triangle dash line, giant component (32.9%) in blue star dash line, and structural failure (0%) in red dot-dash line.

We define three types of failure in transportation network under flooding impact: (i) SF (i.e., road closure due to flood inundation), (ii) FF (i.e., unsatisfied travel speed demand due to traffic slowdown), and (iii) TF due to isolation from GC by (i) and (ii) despite being intact and functional. The GC represents the largest connected cluster where network connectivity remains. Figure 2 shows the temporal variation of different failures and their corresponding GC. The impact of urban flooding can be clearly identified when SF increases during Harvey. A maximum of 2.6% of roads were inundated during Harvey. Meanwhile, FF also increased to its maximum value of 46.3% along with the maximum TF of 30.2%. The coupled effects of these failures led to a sharp drop in the GC to its minimum level of 21.6%. At the

beginning of the post-Harvey phase, because road inundation persisted due to the gradual flood recession (due to the controlled water release from the Barker and Addicks reservoirs), people were still reluctant to commute due to safety concerns. Therefore, the network reaches its maximum connectivity of 39.2%, with both FF and TF dropping to their minimum values of 37.2% and 23.3%, respectively.

Percolation modeling of Harvey flood-disrupted transportation network robustness. We represent the transportation network G at different times t (hourly) as a network $G(V, E, t)$. In a network that has a changing temporal flow (attributes indicating link quality), we can analyze the network at a particular time and
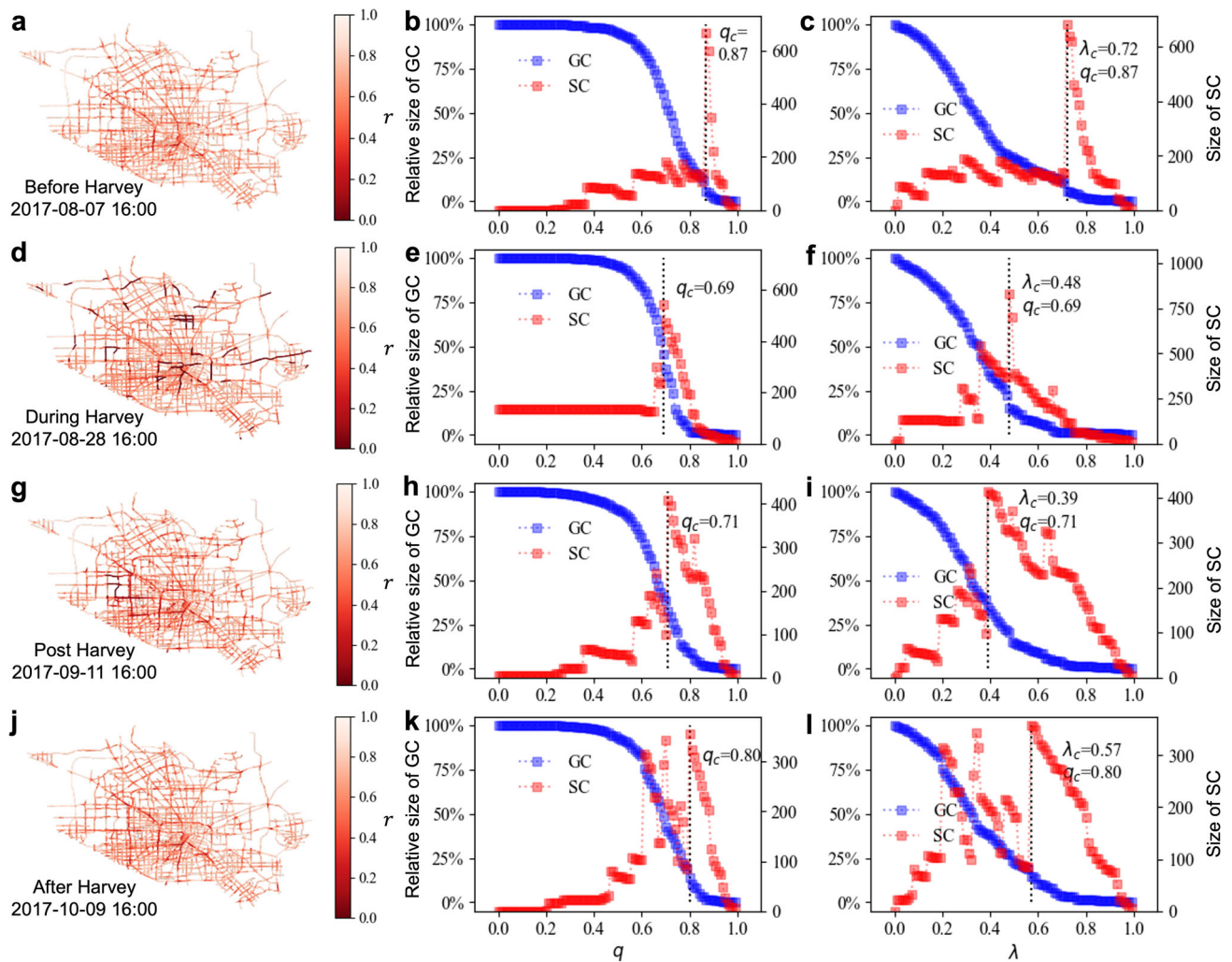
Fig. 3 Percolation analysis on Harris County's transportation network under the influence of flooding caused by Hurricane Harvey. a, d, g, j Transportation network service degradation snapshots before (August 1–24), during (August 25–31), post (September 1–21), and after Harvey (September 22–October 31). **b, e, h, k** Percolation process as a function of link quality threshold q in different phases of Harvey. **c, f, i, l** Percolation process as a function of low link quality percentage λ. The irregular increase of the second giant component (SC) size (red square) is used to identify the critical percolation threshold in the giant component (blue square) phase transition.

examine the network structure and link quality. Each link $i \in E$ corresponds to a road in the transportation network, and each node corresponds to road intersections. We measure the link quality (i.e., traffic condition) for road i at time t based on travel speed ($v_i(t)$) and reference speed (v_i^m) ratio $r_i^t = v_i(t)/v_i^m$. When r_i^t is smaller than a defined threshold q, we consider the road to have low link quality (i.e., congested). In the context of road transportation networks, since users have freedom traveling or communicating within the largest connected cluster, that is, the GC[2], the size of GC is primarily used as a measure of network connectivity[14,31–34]. We remove any link in G with link quality r less than q and examine the GC in the residual network G_q. The critical percolation threshold q_c at which the GC suddenly breaks into smaller components is of particular importance, as it signals the network connectivity loss once link quality drops below q_c[35,36] (see "Methods"). We use the size of SC (second GC) to identify the percolation threshold.

The percolation process on a snapshot of Harris County's transportation network at four different phases of Hurricane Harvey is illustrated in Fig. 3. SF is first overlaid to the network by removing the inundated roads, and FF is then imposed on the

network (see "Methods"). Figure 3d shows that extensive link quality deterioration (i.e., congestion) occurred during Hurricane Harvey. This is because flooding not only caused SF but also resulted in FF due to travel demand shifts (e.g., detours) to other roads and speed reduction due to lane closures in partially flooded areas. Figure 3b, e, h, k demonstrate the percolation process, indicating performance loss (quantified based on the value of the critical threshold for link quality) in the transportation network during Harvey as percolation shows the removal of the links with link quality values less than $q_c = 0.69$ (i.e., congested roads) led to catastrophic network fragmentation (i.e., the breakdown of GC into small components), compared with $q_c = 0.81$ and $q_c = 0.87$ values related to the periods before and after Harvey. However, due to the temporal nature of congestion dynamics, the number of links removed for the same q_c can vary at different times. For example, there can be 60% of link has link quality lower than $q_c = 0.8$ during rush hours, whereas only 30% during regular hours. Removing links based on $q_c = 0.8$ value would suggest different network robustness behaviors at other times. Therefore, considering only q_c in robustness measurement can be misleading. Here, we consider
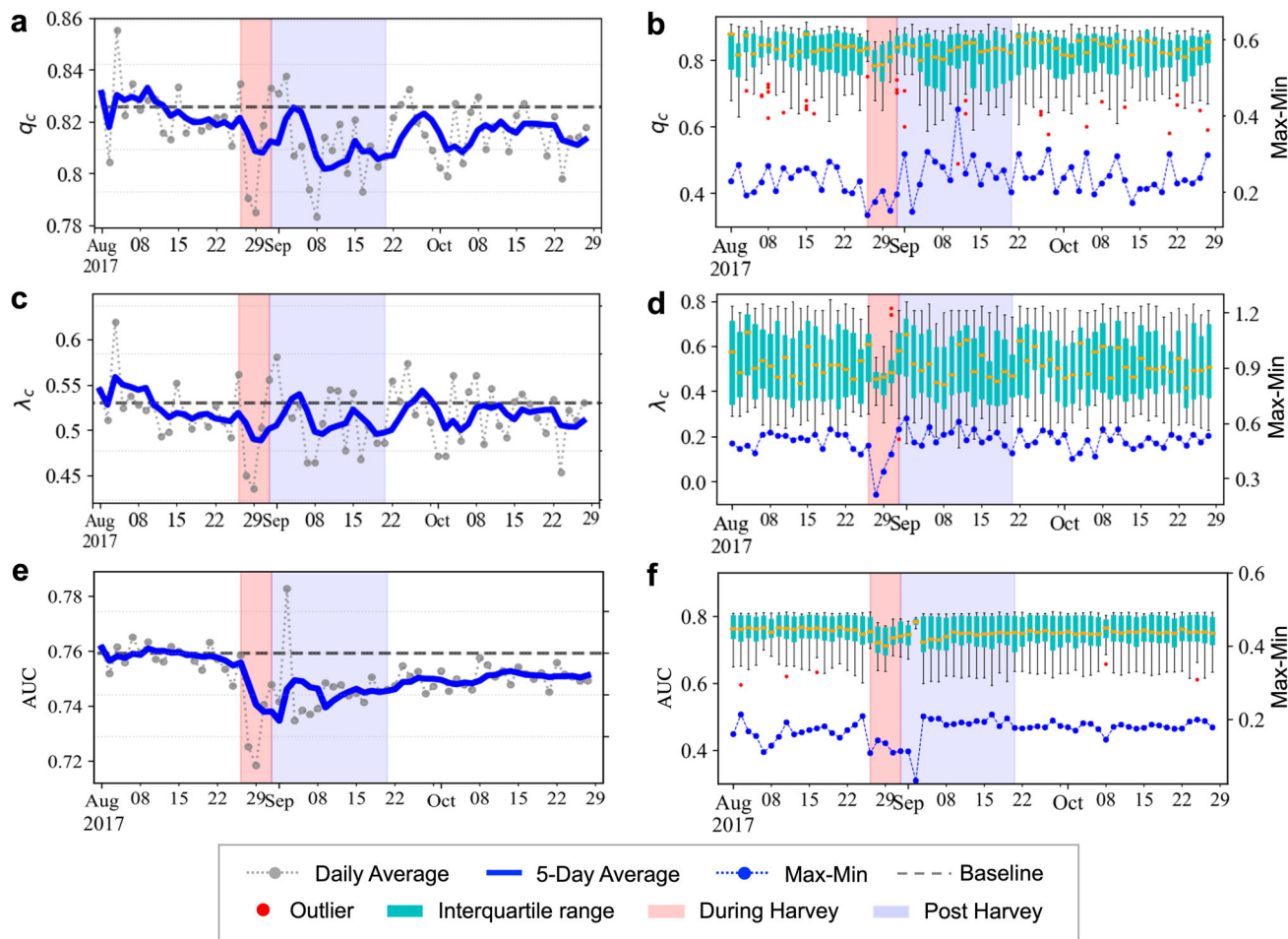
Fig. 4 Temporal variation of percolation critical thresholds q_c and λ_c and area under the curve (AUC) on weekdays. a, **c**, **e** Time series of average q_c, λ_c, and AUC (blue solid lines). The baseline is calculated based on the two-week average values for the period prior to Hurricane Harvey. **b**, **d**, **f** Temporal variation range of q_c, λ_c, and AUC (turquoise bar). Max–min curve (blue dot solid line) is generated by subtracting their maximum and minimum value each day.

additional steps to calculate the exact fraction of links removed in different scenarios to investigate road transportation network robustness under flood-induced compound failures.

Let λ be the fraction of the low-quality (e.g., congested) links removed. At each timestamp t, we ranked the network link based on link quality $r_i(t)$, removed a fixed percentage λ, and examine the GC and SC. Figure 3c, f, i, l show the percolation process as a function of λ. We can see that it would require $\lambda_c = 0.72$ fractions of link removal to have large network connectivity loss before Harvey. However, it only takes $\lambda_c = 0.48$ fractions of the road removal with low link quality (i.e., travel speed is less than reference speed) to disrupt the network connectivity during Harvey. Moreover, we observed that there is only a maximum of 2.6% flood-induced road closure. Since a small fraction of road inundation can lead to such a drastic network robustness change (i.e., 0.24 decrease of λ_c), we conclude that Harris County's transportation network is fragile to flood disruption. Also, λ_c is related to q_c. In fact, there are λ_c fraction of links that have quality less than q_c. By combining both q (i.e., link quality) and λ (i.e., quantity), we can obtain a comprehensive and reliable measurement of network connectivity.

Flood disturbed transportation network stability. The critical threshold fluctuates in temporal networks such as road transportation networks. Figure 4 shows the temporal variation of q_c and λ_c in different phases of Hurricane Harvey. Critical threshold

indicates that removing links whose quality is below q_c or removing λ_c fraction of the low-quality (congested) links will lead to network connectivity loss. The daily average and 5-day moving average of q_c and λ_c both decreased when Hurricane Harvey landed, as illustrated in Fig. 4a, c. Although fewer people commuted when Harvey landed, link quality was still low because travel speed slowed due to safety concerns. The valley in q_c and λ_c during the Harvey period indicates a fragile transportation network in which removal of a small number of roads with low quality led to network connectivity loss. Additionally, we examined the statistical significance of such a drop during Hurricane Harvey. By performing an independent two-sample t-test on q_c and λ_c before and during Harvey, we obtain a p-value of 0.0001 and 0.0014, respectively. As they are all below 1%, we reject the null hypothesis of equal average before and during Harvey. Combining with the results in Fig. 4a, c, we can conclude that Harvey flooding indeed disrupted the network and resulted in severe robustness loss.

Although the critical thresholds increased in the post-Harvey period, the link quality and network robustness did not return to the baseline level. This can be explained by the impaired mobility due to the enormous debris on local roads, such as downed trees and power lines, appliances, electronics, construction and demolition debris, and household hazardous waste, which is reported to take months to remove[37]. To expedite the transportation network robustness recovery, optimization

methods can be developed to prioritize the cleaning of streets that can improve network mobility the most.

Flooding also perturbs link quality stability. Figure 4b, d shows that Hurricane Harvey led to a decrease in q_c and λ_c and a narrower variation range during Harvey. Flooding impacted the q_c and λ_c differently, however, in the post-Harvey phase. Specifically, the interquartile range of q_c was larger in the post-Harvey period than the pre-Harvey period, and the max-min value also shows a large peak in the post-Harvey period. As the critical percolation thresholds, q_c and λ_c, are important indicators of the network robustness, the large max-min value means that the network is less stable during Harvey and in the post-Harvey periods (see Supplementary Fig. 2 for more details); specifically, network fragmentation can happen in a wider range of FF scenarios, which suggests that undesired traffic bottlenecks can happen in various traffic conditions[19]. Figure 4d shows a sudden shrinkage in the interquartile range of λ_c compared with the pre-Harvey condition. The results show that urban flooding has a persistent impact on network robustness stability. This is particularly important as network metastability reveals the bottleneck in the network[18,38], and accurate identification of network metastable state enables the development of corresponding traffic management strategies to ensure premium transportation system efficiency.

The area under the curve (AUC) of the percolation process (see Methods for more details) shows a comprehensive measurement of network robustness. We examined the AUC facing Hurricane Harvey. Figure 4e suggests that the onset of Hurricane Harvey led to the decrease of average AUC, namely network robustness. Despite the receding of floodwater after Harvey, network robustness was not able to fully recover to pre-Harvey condition. Figure 4f shows the fluctuation of the network robustness range. We observed a sudden pattern disruption in the midst and at the beginning of post-Harvey that corresponds to the previous investigation of q_c and λ_c. Also, the max-min range of AUC increases after the disruption, which also suggests the network robustness is unstable after Harvey flooding.

Flood exacerbated transportation network fragility. Modest flood failures can lead to drastic transportation network robustness reduction measured by network connectivity loss. This is attributable to road closures due to flood inundation leading to traffic rerouting, which further burdened the links with low link quality in the network. Figure 5 illustrates the spatial distribution of the three network failures at $q = 0.8$. (See Supplementary Note 2 and Supplementary Figs. 3 and 4 for more detail.)

The failure proportion variation with respect to GC in four different stages of Hurricane Harvey shows the impact of each failure type on the transportation network connectivity. In a case, that travel speed at 80% of the reference speed is considered satisfactory service quality, when no flooding presents (Fig. 5a), FF alone (51.3% link removal) led to 29.5% of the TF and left only 19.2% of roads in the GC. When Hurricane Harvey landed (Fig. 5b), 2.2% flood-induced SF and the latent flood impact resulted in an increase of FF (63.7%) and TF (32.6%), leaving only 1.5% of roads remaining in the GC. Such a large GC reduction due to flooding disruption confirms the amplification effect of the compound structural (i.e., flooding) and functional (i.e., congestion) failures. The network starts to recover in the post-Harvey period (Fig. 5c) with only 0.1% of links having SF and 13.2% of links present in the GC, but still, the robustness of the network was below the pre-Harvey level. As time passed and the city recovered from the flood impacts, the transportation network performance gradually approached the pre-Harvey condition (Fig. 5d).

Relationship between network failures and network connectivity. To better understand the compound failure dynamics over the course of Hurricane Harvey, we conducted a regression analysis to quantify their relationships. Figure 6a–c show the empirically fitted $y \sim \log(x)$ relationships between SF and FF, TF, and GC. We can see that there is a nonlinear relationship between them. In particular, in the lower range of SF, a small increase can lead to a large increase in FF and TF, which eventually will lead to extensive network connectivity loss. Figure 6d–f show the relationship between FF and GC in the presence versus absence of flooding. The impact of link quality on GC diminishes when flooding occurs (during & post-Harvey) and bounces back when flood recedes (post-Harvey). However, the network status does not return to pre-Harvey level immediately after the recession of floodwater. This delay could be due to changes in people's movement patterns in the aftermath of flooding. Although flooding exacerbated network service quality and increased congestion, FF became less dominant in reducing the GC since SF and TF dramatically increased. This set of results reveals that flooding exacerbates other types of network failures and creates catastrophic impacts on network connectivity.

We further illustrated the impact of flooding on network robustness by comparing the empirical scenario with two synthetic cases: no-flooding and random-flooding. The percolation process of a transportation network G in a flood scenario r encapsulates f flooding link removal and $\lambda - f$ under-serving link removal if more than f links are removed, where λ is the total fraction of links that requires removal. By manipulating f (see Methods for details), we obtained no-flooding ($f = 0$) and random-flooding (random f) scenarios. In doing so, we could reveal the extent to which f flooding can impact road network connectivity by subtracting empirical flooding percolation AUC from synthetic flooding scenarios (e.g., no-flooding and random flooding). Figure 7a gives an illustration of how we measure the impact of the flood. At a given q, if the network presents a more robust behavior (i.e., a larger size of GC) under synthetic flooding scenario than the empirical flooding scenario, a positive value is obtained. A positive area indicates that the network is more robust under synthetic flooding, compared with flooding in reality. Analogously, a negative value implies that the synthetic flooding weakens the network robustness more than the empirical flood. By aggregating the differences of robustness value across all q values, namely, summation of the positive and negative area, we obtain the total flood impact.

We examined the road network from August 25 to September 8, when flooding appeared to be heaviest (Fig. 2). Figure 7b shows that by excluding the flooding, network robustness shows an oscillating behavior where both superior and inferior robustness can occur, while Fig. 7c shows that random flooding is worse than empirical flooding. One plausible reason is that the flooding-induced failure is between localized attack and random failures that delays the disaggregation of the giant component. By dissecting flooding into different phases, we can see that flooding impact is 0 on August 25 (Fig. 7d), because flooding is minimal at the beginning of Hurricane Harvey (Fig. 2). As flooding accelerates during August 25–30, all positive AUC difference in Fig. 7e shows that excluding flooding results in higher robustness, suggesting that flooding impact on network robustness becomes severe. As flooding dies down during August 25–September 4 (Fig. 2), Fig. 7f shows flooding is not the major factor affecting network robustness, but rather traffic dominates. This is likely caused by traffic resurrection post-Harvey. When minimum flooding is sustained on the network during September 5–8 (Fig. 2), flooding and traffic show equal impact on network robustness as AUC differences present a random behavior Fig. 7g.
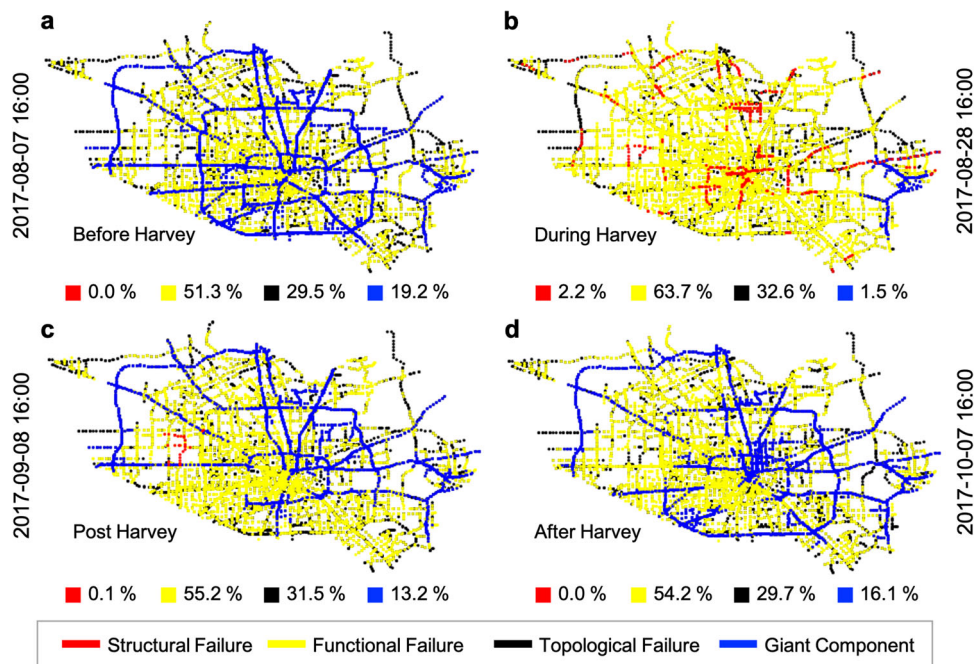
Fig. 5 Spatial distribution of network failures in the afternoons with threshold $q = 0.8$. The same weekday (Monday) and time (16:00) are selected for the illustration. **a** Transportation network before Harvey in which functional failure (yellow line) is the leading cause of network connectivity loss. **b** When Hurricane Harvey landed, flooding (i.e., structural failure in red line) exacerbated the functional failure (i.e., travel speed reduction) and topological failure (black line), leading to large-scale network fragmentation (i.e., giant component reduction in blue line). **c** Immediate post-Harvey recovery with part of transportation network remaining flooded. **d** Transportation network long-term recovery after Harvey.
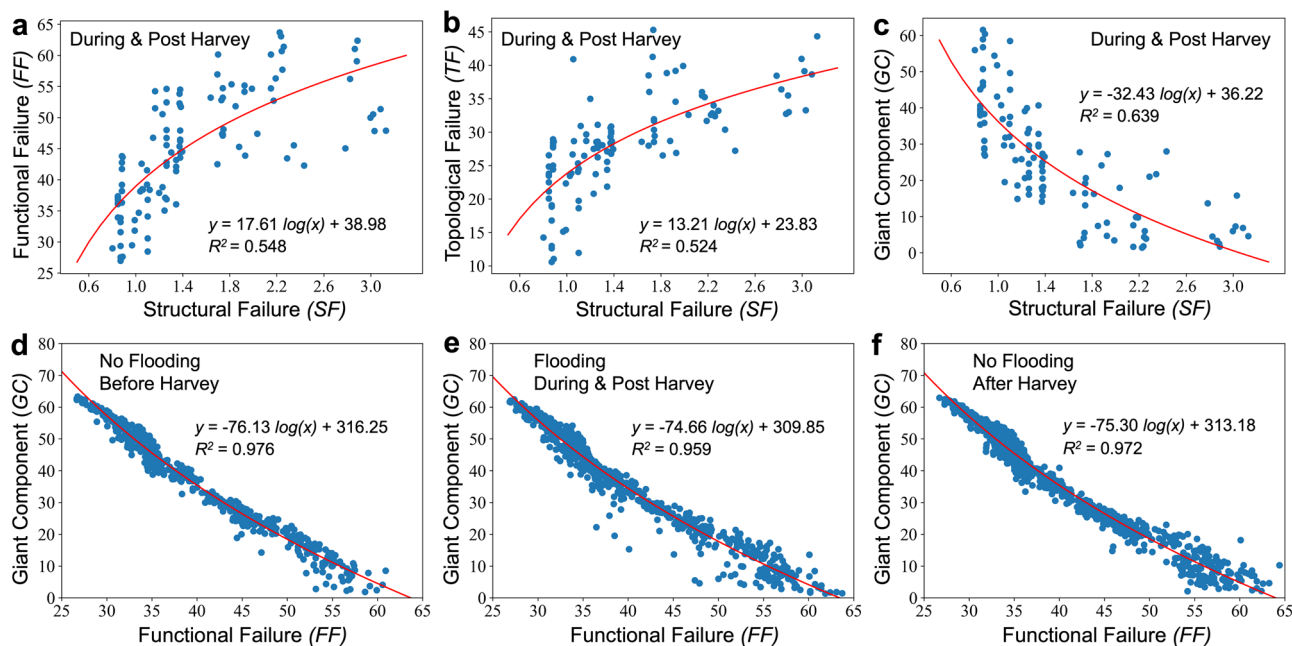
Fig. 6 Unveiling the relationship among structural failure (SF), functional failure (FF), topological failure (TF), and giant component (GC). We use $q = 0.8$ for the illustrative purpose. We use a $y = a \sim \log(x) + b$ to fit the empirical failure data. **a, b, c** Relationship between SF and FF, TF, and GC. Only non-negligible flooding (i.e., SF larger than 0.5%) during the time period 6:00 a.m. to 8:00 p.m. is considered. (See Supplementary Note 3 and Supplementary Fig. 5 for more details.) **d–f** Relationship between FF and GC in different stages of Hurricane Harvey.

Discussion

This study revealed that urban flooding triggers compound failures leading to network robustness instability and catastrophic collapse in road transportation networks. We show that the impact of the flood is not limited to road inundation but extends to the link quality change. The results illustrate that the need for maintaining a satisfactory level of link quality and network connectivity is important for enhancing performance in flood-impacted transportation networks. To quantify the relationship between the compound network failures and their impact on transportation network connectivity, we utilized high-resolution traffic and flood data and employed percolation modeling to
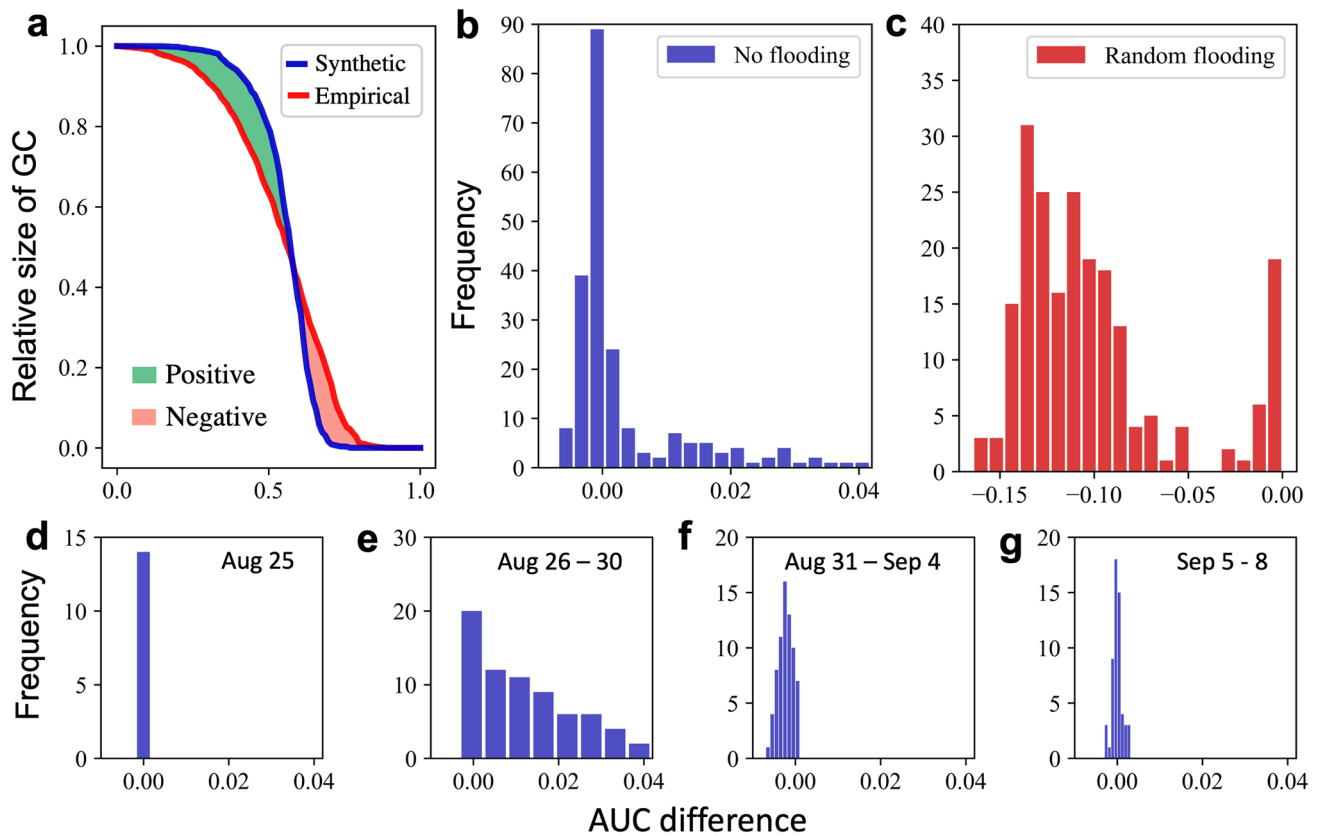
Fig. 7 Flood impact comparison between empirical and synthetic no-flooding and random-flooding scenarios. a Schematic illustration for robustness AUC difference calculation. The total flood impact difference is the summation of the positive (green shade) and negative (red shade) areas. **b** Histogram of AUC difference between no-flooding and empirical-flooding case (blue bar). **c** Histogram of AUC difference between random flooding and empirical flooding case (red bar). **d**–**g** The AUC difference frequency during different time frames.

characterize flood-induced structural and functional failures, and used Harris County in the scenario of 2017 Hurricane Harvey as a case study.

Three failures affect the transportation network during urban flooding: SF (flooding), FF (congestion), and TF (indirect). We show that modest flood-induced SF would amplify the other failures by reducing the number of viable roads for travel. The redistribution of travel demand would increase the FF in other parts of the network (Fig. 3). More importantly, many critical roads are often built near river basins where human activities are popular[2]. Urban flooding often inundates highway ramps and bridge underpasses, failure of which will cut off connections between communities and the giant component (Fig. 5a, b). In addition, the impact of flooding is long-lasting and disturbs the network stability (Fig. 4). Our investigation and quantification of compound failures (Fig. 6) show that small SF will exacerbate the FF and TF and result in a huge drop in GC, which reflects the extreme vulnerability of the transportation network in the face of flood perturbations.

The findings of this study have profound implications since cities are facing growing risks of urban flooding and congestion. The results show the collision of these two stressors-urban floodings and population growth-would have catastrophic impacts on transportation networks when considering the compound structural and functional failures. Hence, long-term transportation development and flood risk reduction plans should consider the compound impacts of these failures and adopt measures and make investments to enhance the robustness of road transportation networks in preparation for future urban growth and exacerbated flood risks. For example, measures (such

as public transportation) that alleviate traffic congestion on road segments could greatly contribute to network robustness during flooding. Congestion reduction measures could prevent the amplification of the effects of urban flooding on-road transportation networks. Also, hazard mitigation plans should account for functional failures during and in the aftermath of floods to examine the access of different populations to critical facilities. The current approaches, however, primarily focus on structural failures. Our study bridges the gap by considering flood disruption on physical structure, flow transport, and topological integrity. The proposed analysis procedure can also be applied in other disruption scenarios, such as snowstorms, cyberattacks, and extreme wind hazards.

The proposed formulation and analysis of the Harris County road network during hurricane Harvey demonstrate that modest flooding can induce catastrophic traffic service failure. Extending the promising results of this research to other cities with different geological features (e.g., rivers, mountains), different infrastructure networks (e.g., power, water, and telecommunication network), and different types of disaster events (e.g., snowstorms, tornadoes, and strong winds) requires harnessing more meteorological and mobility data, which will be addressed in our future research. Moreover, compound infrastructure failure (e.g., power outage-induced during the 2021 winter storm in Texas and 2021 Hurricane Ida evacuation during COVID) and travel behavior change during special events (e.g., concerts and sports events) can further exacerbate traffic meltdown and cause extensive loss of road service. In addition, people's mobility and accessibility to critical facilities, particularly socially vulnerable populations, are vital in ensuring community well-being. Future research can

investigate how disaster-disrupted service affects community resilience at scale and how we can strategically develop policy to mitigate such adverse impact. Integration of these factors into future research design can greatly improve our understanding of structural and FFs interplay and their impact on system stability.

Conclusions

This paper examines the impact of compound structural and FFs on network resilience[39] in the case of the Hurricane Harvey flooding-inundated and -immobilized transportation networks. We conclude that floods can exacerbate transportation network failure. The critical percolation threshold of network robustness shows the recovery behavior (disruption, reduction, and bounce-back) throughout all phases of Hurricane Harvey. Specifically, we discover that 2.2% of flood-induced compound failure can cause a 17.7% decrease in the GC size of the transportation network. In addition, we reveal that there is a non-linear relationship among structure failure (flooding), function failure (heavy traffic), TF (indirect failure), and network robustness (GC). This is supported by the flood impact between different engineered flooding scenarios, where a less robust transportation network is presented in the flood-impacted traffic scenario than in the traffic-only scenario. Nonetheless, network robustness is the lowest in the case of random flooding. The findings of this paper shed light on the transportation network meta-stability in facing different types of network disruptions and provide a holistic approach for examining the mobility and accessibility issue during floods.

Methods

Link quality derivation. The data used in this paper are 15-min interval travel speed data at each major road in Harris County for August, September, and October 2017. Link quality is a metric that is used for describing the travel condition for each link (see Supplementary Note 1 for more details). Compared with a link's speed limit, the lower the travel speed is at each time interval, the more severe the congestion and thus lower travel performance is on the road. Instead of using maximum speed as the speed limit, however, we created a speed profile for each road and used its 95 percentile[19] as its reference speed. (See Supplementary Fig. 1 for more detail.) The link quality of road i at time t is expressed as a ratio, which is defined as

$$r_i^t = \frac{v_i(t)}{v_i^m} \tag{1}$$

where $v_i(t)$ represents the travel speed of road i at time t, which is a time-varying property of the road. v_i^m represents the reference speed of road i; it is an intrinsic value of the road.

Network construction. The baseline network starts with a network that contains 19,712 links and 15,390 nodes. To construct the network at time t, we first removed roads that were inundated. This is done by checking and removing roads marked as closed. Second, we examined if the road meets the travel criterion. We use link quality threshold $q \in [0, 1]$ to represent the acceptable travel condition. A small q indicates the road is heavily congested. To construct a temporal transportation network at time t with the acceptable quality level of q, we first derive the link quality of each road. When $r_i^t < q$, we consider the road is congested and removed from the network; when $r_i^t \geq q$, we consider the road as functional and mark it as occupied in the network, as shown in Eq. (2).

$$\begin{cases} 1 \ (\text{Flowing}) & r_i(t) \geq q \\ 0 \ (\text{Congested}) & r_i(t) < q \end{cases} \tag{2}$$

In doing so, we have a sequence of binary link indices at time t, representing whether the link is functioning in the network. To generate the transportation network at time t with specified q, we apply Eq. (2) to each road and collect the functional roads to build the network $G(t, q)$ based on their geographic location.

Flooding scenarios engineering. We define f as the fraction of flooded links and λ as the fraction of total links removed. In a flood scenario z, when $\lambda > f$, we remove f fraction of flooded links and $\lambda - f$ fraction of low-quality links based on their quality r rank; and when $\lambda < f$, we only remove f fraction of flooded links. The AUC represents the robustness of the network. AUC is defined as

$$\text{AUC} = \frac{1}{T} \sum_{q=1}^{T} s(\lambda) \tag{3}$$

where T is the total number of steps involved in the percolation process, and $s(\lambda)$ is the fraction nodes in the GC as the results of removing the first λ fraction of low-quality nodes. Similarly, if we are removing nodes based on link quality threshold q, the equation will be substituted with $s(q)$, representing the fraction nodes in the GC as a function of removing nodes that are below congestion level q. The $1/T$ normalizes the result so that the robustness of networks of different sizes can be compared[40–42]. The area under the curve is a comprehensive robustness performance measure during all possible traffic congestion scenarios[40]. We use this measure to avoid the situation where two processes show the same critical percolation threshold λ_c or q_c[34,43] but display different robustness behavior at other λ or q values.

The principle of flooding scenario engineering is to ensure the total fraction of removed links λ is the same. We only manipulate the failure sequence of the flooded links to create different flood scenarios and keep other links unchanged. In the original flooding scenario, we remove the f fraction of flooded links first (because they have the quality of $r = 0$), and then we proceed to remove other $\lambda - f$ low quality (i.e., congested) links to make up the λ total removal.

To derive the no-flooding scenario, we find the maximum link quality $r_{\max}$ at the time and assign the f fraction of flooded links with $r_{\max}$. Then, we proceed with removing λ fraction of roads based on their link quality. In doing so, we make sure the flooded links are removed at the end of the percolation simulation, creating a flood percolation phenomenon that is equivalent to a no-flooding scenario $f = 0$.

For a random flooding scenario, we first assign the flooded links the maximum link quality to enforce their removal at the end of the percolation simulation. At the same time, we randomly select f fraction of links and remove them first to create the random flooding case. Then, we remove $\lambda - f$ (if $\lambda > f$) or 0 (if $\lambda < f$) fraction to make up the total λ fraction of link removal. In doing so, we acquire both no-flooding and random-flooding scenarios.

Percolation simulation. The percolation process involves removing links that do not meet the criteria, i.e., the link quality is below a threshold q_c. After removing these unqualified links, the initially fully connected network may break into multiple components depending on the thresholds. The largest connected cluster, namely, the GC, can well reflect the connectivity or the fragmentation of the road transportation network[2]. Therefore, we use the GC, namely, the largest connected component, as the metric to represent system navigability in facing failures[14,19,33,34,36,44,45]. To conduct the percolation simulation at time t with proper q, we first constructed the network with the aforementioned methods. Next, we apply different flooding scenarios to the network. Finding the GC requires enumerating through all the connected clusters and selecting the largest one. The search of a connected component can be achieved by using the either breadth-first search or depth-first search algorithm. When a connected component is found but the total size of the connected component is smaller than the whole network, we selected a new link that has not been removed or searched and conducted the previous procedure again, until the summation of connected components and removed flooded links equals the whole network. We ranked the size of the connected components; the largest connected component is the GC. The second-largest connected component is used to indicate the phase transition of the percolation process, where the GC suddenly fragments into smaller components. We used the Python module NetworkX to conduct the aforementioned percolation analysis. The analytical solution can be found in our earlier paper[2].

Data availability

Code availability

References

1. Zhang, L. et al. Scale-free resilience of real traffic jams. *Proc. Natl Acad. Sci. USA* **116**, 8673–8678 (2019).
2. Wang, W., Yang, S., Stanley, H. E. & Gao, J. Local floods induce large-scale abrupt failures of road networks. *Nat. Commun.* **10**, 1–11 (2019).
3. Li, D., Zhang, Q., Zio, E., Havlin, S. & Kang, R. Network reliability analysis based on percolation theory. *Reliab. Eng. Syst. Safety* **142**, 556–562 (2015).
4. Korkali, M., Veneman, J. G., Tivnan, B. F., Bagrow, J. P. & Hines, P. D. Reducing cascading failure risk by increasing infrastructure network interdependence. *Sci. Rep.* **7**, 1–13 (2017).

5. Albert, R., Albert, I. & Nakarado, G. L. Structural vulnerability of the North American power grid. *Phys. Rev. E* **69**, 025103 (2004).
6. Daqing, L., Yinan, J., Rui, K. & Havlin, S. Spatial correlation analysis of cascading failures: congestions and blackouts. *Sci. Rep.* **4**, 1–6 (2014).
7. Saberi, M. et al. A simple contagion process describes spreading of traffic jams in urban networks. *Nat. Commun.* **11**, 1–9 (2020).
8. Aerts, J. C. et al. Integrating human behaviour dynamics into flood disaster risk assessment. *Nat. Clim. Change* **8**, 193–199 (2018).
9. Nofal, O. M. & Van De Lindt, J. W. Understanding flood risk in the context of community resilience modeling for the built environment: research needs and trends. *Sustain. Resil. Infrastruct.* **0**, 1–17 (2020).
10. Singh, P., Sinha, V. S. P., Vijhani, A. & Pahuja, N. Vulnerability assessment of urban road network from urban flood. *Int. J. Disaster Risk Reduct.* **28**, 237–250 (2018).
11. Gori, A. et al. Accessibility and recovery assessment of Houston's roadway network due to fluvial flooding during hurricane Harvey. *Nat. Hazards Rev.* **21**, 04020005 (2020).
12. Chen, X.-Z., Lu, Q.-C., Peng, Z.-R. & Ash, J. E. Analysis of transportation network vulnerability under flooding disasters. *Transp. Res. Rec.* **2532**, 37–44 (2015).
13. Holling, C. S. Resilience and stability of ecological systems. *Ann. Rev. Ecol. Syst.* **4**, 1–23 (1973).
14. Gao, J., Barzel, B. & Barabási, A.-L. Universal resilience patterns in complex networks. *Nature* **530**, 307–312 (2016).
15. Pregnolato, M., Ford, A., Glenis, V., Wilkinson, S. & Dawson, R. Impact of climate change on disruption to urban transport networks from pluvial flooding. *J. Infrastruct. Syst.* **23**, 04017015 (2017).
16. Lu, Q.-C. & Peng, Z.-R. Vulnerability analysis of transportation network under scenarios of sea level rise. *Transp. Res. Rec.* **2263**, 174–181 (2011).
17. Demirel, H., Kompil, M. & Nemry, F. A framework to analyze the vulnerability of European road networks due to Sea-Level Rise (SLR) and sea storm surges. *Transp. Res. Part A* **81**, 62–76 (2015).
18. Zeng, G. et al. Switch between critical percolation modes in city traffic dynamics. *Proc. Natl Acad. Sci. USA* **116**, 23–28 (2019).
19. Li, D. et al. Percolation transition in dynamical traffic network with evolving critical bottlenecks. *Proc. Natl Acad. Sci. USA* **112**, 669–672 (2015).
20. Dong, S., Esmalian, A., Farahmand, H. & Mostafavi, A. An integrated physical-social analysis of disrupted access to critical facilities and community service-loss tolerance in urban flooding. *Comput. Environ. Urban Syst.* **80**, 101443 (2020).
21. Dong, S., Wang, H., Mostafizi, A. & Song, X. A network-of-networks percolation analysis of cascading failures in spatially co-located road-sewer infrastructure networks. *Physica A* **538**, 122971 (2020).
22. Dong, S. et al. Integrated infrastructure-plan analysis for resilience enhancement of post-hazards access to critical facilities. *Cities* **117**, 103318 (2021).
23. Faturechi, R. & Miller-Hooks, E. Measuring the performance of transportation infrastructure systems in disasters: a comprehensive review. *J. Infrastruct. Syst.* **21**, 04014025 (2015).
24. Fan, C., Jiang, X. & Mostafavi, A. A network percolation-based contagion model of flood propagation and recession in urban road networks. *Sci. Rep.* **10**, 1–12 (2020).
25. Dong, S., Wang, H., Mostafavi, A. & Gao, J. Robust component: a robustness measure that incorporates access to critical facilities under disruptions. *J. R. Soc. Interface* **16**, 20190149 (2019).
26. Chopra, S. S., Dillon, T., Bilec, M. M. & Khanna, V. A network-based framework for assessing infrastructure resilience: a case study of the london metro system. *J. R. Soc. Interface* **13**, 20160113 (2016).
27. Ganin, A. A. et al. Resilience and efficiency in transportation networks. *Sci. Adv.* **3**, e1701079 (2017).
28. Hamedmoghadam, H., Jalili, M., Vu, H. L. & Stone, L. Percolation of heterogeneous flows uncovers the bottlenecks of infrastructure networks. *Nat. Commun.* **12**, 1–10 (2021).
29. Callaway, D. S., Newman, M. E., Strogatz, S. H. & Watts, D. J. Network robustness and fragility: percolation on random graphs. *Phys. Rev. Lett.* **85**, 5468 (2000).
30. Cohen, R. et al. Resilience of the internet to random breakdowns. in *The Structure and Dynamics of Networks*, 507–509 (Princeton University Press, 2011).
31. Buldyrev, S. V., Parshani, R., Paul, G., Stanley, H. E. & Havlin, S. Catastrophic cascade of failures in interdependent networks. *Nature* **464**, 1025–1028 (2010).
32. Dong, S., Mostafizi, A., Wang, H., Gao, J. & Li, X. Measuring the topological robustness of transportation networks to disaster-induced failures: a percolation approach. *J. Infrastruct. Syst.* **26**, 04020009 (2020).
33. Shao, S., Huang, X., Stanley, H. E. & Havlin, S. Percolation of localized attack on complex networks. *N. J. Phys.* **17**, 023049 (2015).
34. Gao, J., Buldyrev, S. V., Stanley, H. E. & Havlin, S. Networks formed from interdependent networks. *Nat. Phys.* **8**, 40–48 (2012).
35. Havlin, S. & Cohen, R. *Complex Networks: Structure, Robustness and Function* (Cambridge University Press, 2010).
36. Barabási, A.-L. *Network Science* (The Royal Society Publishing, 2016).
37. Ibrahim, A. After Harvey, another mammoth challenge for flooded areas: getting rid of mountains of trash. https://www.texastribune.org/2017/09/22/ (2017).
38. Zeng, G. et al. Multiple metastable network states in urban traffic. *Proc. Natl Acad. Sci. USA* **117**, 17528–17534 (2020).
39. Liu, X. et al. Network resilience. Preprint at *arXiv* https://arxiv.org/abs/2007.14464 (2020).
40. Schneider, C. M., Moreira, A. A., Andrade, J. S., Havlin, S. & Herrmann, H. J. Mitigation of malicious attacks on networks. *Proc. Natl Acad. Sci. USA* **108**, 3838–3841 (2011).
41. Alessandro, V. Complex networks: the fragility of interdependency. *Nature* **464**, 984–985 (2010).
42. Iyer, S., Killingback, T., Sundaram, B. & Wang, Z. Attack robustness and centrality of complex networks. *PloS ONE* **8**, e59613 (2013).
43. Bunde, A. & Havlin, S. Fractals and disordered systems, Percolation i. (2012).
44. Gao, J., Buldyrev, S. V., Havlin, S. & Stanley, H. E. Robustness of a network of networks. *Phys. Rev. Lett.* **107**, 195701 (2011).
45. Liu, X. et al. Robustness and lethality in multilayer biological molecular networks. *Nat. Commun.* **11**, 1–12 (2020).

Acknowledgements

Author contributions
S.D., X.G., A.M., and J.G. conceived the experiment(s), S.D. and X.G. performed the simulation, S.D., X.G., and J.G. analyzed the results. A.M. supervised the project, revised the paper, collected the data, and secured funding support. S.D. and J.G. led the writing of the paper. All authors participated results discussion and agreed to the published version of the paper.

Competing interests
The authors declare no competing interests.

Additional information